

Borane-catalysed cyclodepolymerization of CO₂-derived polycarbonates†

Mikhailey D. Wheeler  and Francesca M. Kerton *

Received 24th April 2025, Accepted 20th May 2025

DOI: 10.1039/d5fd00050e

The Lewis acidic borane tris(pentafluorophenyl)borane, B(C₆F₅)₃ or BCF, has been found to selectively depolymerize polycarbonates to their corresponding cyclic carbonates without the need of a co-catalyst. Depolymerizations of poly(propylene carbonate) (PPC) and poly(cyclohexene carbonate) (PCHC) in toluene were studied with varying catalyst loadings and temperatures. Good conversions to the respective cyclic carbonates were observed down to 2.5 mol% BCF and at temperatures down to 75 °C. No conversion was observed under solvent-free or liquid-assisted grinding conditions in a mixer mill. Kinetic studies *via in situ* infrared spectroscopy of the system showed an activation energy of 50.2 ± 6.7 kJ mol⁻¹ for PPC and 83.5 ± 1.7 kJ mol⁻¹ for PCHC. Entropy of activation values were found to be -190.6 ± 18.4 J K⁻¹ mol⁻¹ for PPC and -114.7 ± 3.8 J K⁻¹ mol⁻¹ for PCHC. Initial rates of conversion were significantly faster for PPC than PCHC. Aliquots were taken from reaction mixtures and analyzed *via* ¹H NMR spectroscopy and gel permeation chromatography to understand the reaction mechanism, which was found to occur *via* chain-end backbiting rather than random chain scission. Depolymerization attempts were performed on systems containing various additives/impurities including poly(bisphenol A carbonate), H₂O and CO₂. H₂O was seen to inhibit the reaction. Therefore, it was not surprising that a commercial polycarbonate-diol did not depolymerize under the reaction conditions explored.

Introduction

Chemical recycling of polymers to monomers is an attractive route to creating a circular plastics economy which will contribute to improving waste management issues and minimizing environmental impacts.^{1,2} Nearly 500 million metric tons of plastic are produced every year yet only a small percentage (16% in Canada as of 2022) is recycled back to usable products.^{3,4} Still, current recycling methods are typically inefficient, that is, they are energy intensive and/or produce polymers of diminished value (*e.g.*, mechanical or thermal recycling).⁵ The cyclodepolymerization (CDP) of polycarbonates to their cyclic monomers is a large area

Department of Chemistry, Memorial University, St. John's, NL, A1B 3X7, Canada. E-mail: fkerton@mun.ca

† Electronic supplementary information (ESI) available: NMR spectra and *in situ* FTIR data. See DOI: <https://doi.org/10.1039/d5fd00050e>



of research where two pathways emerge: the formation of cyclic carbonates or the closed-loop depolymerization back to epoxides and CO₂.

Polycarbonates, which can be formed from the ring-opening copolymerization (ROCOP) of epoxides and CO₂, can often be resistant to degradation due to high thermal stability and rigidity, even when considered 'biodegradable'. This creates the need for alternative strategies for polycarbonate recycling. Some of the most exciting results have recently been obtained on conversion of such polymers to their original monomers (epoxides and carbon dioxide).^{1,6–11} For example, McGuire *et al.* have demonstrated the chemical recycling of CO₂-based polycarbonates to monomers in the solid state with a heterodinuclear Mg(II)Co(II) catalyst.¹¹ However, this does not mean that other chemical recycling routes for polycarbonate repurposing are not without merit.

Previous work by us and others has found that organoboranes are effective catalysts for the copolymerization of CO₂ and epoxides.^{9,12–28} Specifically, we have shown that triphenylborane (BPh₃), a Lewis acidic borane, in combination with suitable Lewis basic co-catalysts (neutral or anionic) can catalyse the formation of polycarbonates from epoxides (cyclohexene oxide (CHO)) and CO₂.¹² This catalyst system is also capable of ROCOP of epoxides and anhydrides to produce polyesters, and upon sequential addition of carbon dioxide can yield polyester-*block*-polycarbonates.¹³ The more Lewis acidic borane, tris(pentafluorophenyl)borane (BCF), was found to be inactive in these ROCOP reactions but subsequent studies showed that it could (in the absence of a nucleophile) degrade polycarbonates or polycarbonate blocks to cyclic carbonate products. It was found that BCF could degrade them to cyclic carbonates in CH₂Cl₂ at 130 °C.¹³

Herein, we describe more detailed studies of BCF as a CDP catalyst for polycarbonates made from epoxides and CO₂ in the absence of co-catalysts under relatively mild conditions (2.5 mol% BCF, 2 h, 105 °C in toluene). To our knowledge, these are the first examples of an arylborane acting as a CDP catalyst.

Experimental

General experimental conditions and chemicals

Unless otherwise stated, all experimental procedures were performed using an MBraun Labmaster glovebox or under dry oxygen-free nitrogen using Schlenk techniques. Cyclohexene oxide (CHO), poly(bisphenol A carbonate) (PBPAC), poly(propylene carbonate) (PPC) (¹H NMR spectrum, Fig. S1†), and propylene carbonate (PC) were purchased from Sigma-Aldrich. CHO was dried over CaH₂ and distilled prior to use. PBPAC, PPC, and PC, were used as received. BCF and BPh₃ were purchased from Strem Chemicals and used as received. Bis(triphenylphosphine)iminium chloride (PPNCl) was purchased from Alfa Aesar and recrystallized prior to use. All solvents used were dried and degassed using an MBraun Manual Solvent Purification system.

Instrumentation

¹H NMR spectra were obtained using either a Bruker Avance 300 MHz spectrometer or a Bruker NEO 500 MHz spectrometer at 298 K in CDCl₃ purchased from Cambridge Isotope Laboratories, Inc. ¹¹B NMR spectra were collected on a Bruker NEO 500 MHz spectrometer at 298 K in dry CDCl₃. For kinetic



measurements, a diamond sensor (DiComp) dip probe was connected to a ReactIR 15 base unit (Mettler-Toledo) through a DST Fiber Conduit (Fig. S4 and S5†). The probe was cleaned with acetone or dichloromethane before and after each experiment and calibrated before each run. Any polymerization reactions were performed using a 100 mL stainless steel reactor vessel (Parr Instrument Company) equipped with a mechanical stirrer and a heating mantel. The vessel was baked at 100 °C under vacuum overnight prior to any experiment. Gel permeation chromatography (GPC) analyses were performed using a miniDawn TREOS light scattering detector, a Viscostar-II viscometer, and a Optilab T-REX differential refractive index detector (Waters|Wyatt Technologies) connected to an Agilent Infinity 1260 HPLC system equipped with two Phenogel 103 Å 300 × 4.60 mm columns with THF as the eluent. Samples were prepared in tetrahydrofuran (THF) at a concentration of 4 mg mL⁻¹, filtered through a 0.2 µm PTFE syringe filter, and analyzed at a flow rate of 0.3 mL min⁻¹ at 25 °C. M_n and D were calculated using the Wyatt ASTRA software with d_n/d_c values acquired *via* off-line analysis.

Synthesis of poly(cyclohexene carbonate)

71.5 mg of BPh₃ and 169.6 mg of PPNCl were combined and dissolved in approximately 5 mL CH₂Cl₂ and injected into a pressure vessel (under nitrogen). The CH₂Cl₂ was then removed *via* vacuum and 5.80 g CHO was injected with stirring (such that CHO : PPNCl : BPh₃ was 200 : 1 : 1). The vessel was pressurized to 40 bar CO₂ and heated to 60 °C for 24 h. The vessel was then cooled, and the mixture dissolved in CH₂Cl₂ and the polymer precipitated out with cold acidified methanol (5% HCl), and the polymer was characterized by ¹H NMR spectroscopy (Fig. S2†) and GPC.

Typical BCF catalyzed depolymerization experiment

~500 mg of polymer was added to a 100 mL multi-necked round-bottomed flask equipped with an FTIR dip probe under an N₂ flush. An appropriate volume of dry toluene was added to the flask and the mixture was heated and stirred until the polymer was fully dissolved. Once the desired temperature was achieved, an appropriate amount of standard BCF solution (~60 mg per mL BCF in toluene, from a total volume of 20 mL) was taken from the glovebox and added to the flask *via* syringe under N₂ flush and monitoring *via in situ* FTIR spectroscopy was started. Aliquots were taken (under N₂ flush) at 15, 30, 60, 90, and 120 min, quenched with a drop of acidified methanol, and analyzed by ¹H NMR spectroscopy (*e.g.* Fig. S3†) and GPC.

Results and discussion

Depolymerization of poly(propylene carbonate)

The CDP of poly(propylene carbonate) (PPC) is a relatively understudied area. There exist few metal-based examples to degrade PPC into its cyclic counterpart, propylene carbonate (PC). ZnEt₂-based catalyst systems were reported by Kuran *et al.* to promote cyclization of PPC in moderate yields.^{29,30} In 2012, Darensbourg and coworkers studied an anion assisted depolymerization with a (salen)CrCl catalyst.³¹ Recently, both Enthaler *et al.* and Gallin *et al.* studied different ZnCl₂-



Table 1 Cyclodepolymerization of PPC under varying catalyst loading and temperature conditions^a

Reaction scheme: $\left[\text{C(CH}_3\text{)}_2\text{CH}_2\text{OOC(CH}_2\text{)}_2\text{O} \right]_n \xrightarrow[\text{toluene, 75-105 } ^\circ\text{C, 2 h}]{\text{2.5-10 mol\% BCF}} \text{PC}$

Entry	BCF (mol%)	<i>T</i> (°C)	<i>M_n</i> ^b (kDa)	<i>D</i>	% PC yield ^{c,d}
1	5	75	40.3	7.12	34
2	5	85	24.1	5.08	61
3	5	90	13.6 ^d	2.40	72
4	5	95	16.2	5.79	81
5	5	105	11.6 ^d	3.21	92
6	10	105	10.8 ^d	4.10	96
7	2.5	105	12.2 ^d	3.60	49

^a Conditions: starting PPC molecular weight (*M_n*) was measured to be 51.4 kDa (*D* = 3.93), catalyst loadings were determined with respect to the repeat unit molar mass of the polymer. All reactions performed in 20 mL toluene for 2 h under nitrogen. ^b Molecular weights of aliquots determined by GPC in THF as the eluent. *M_n* and *D* were calculated using the Wyatt ASTRA software with *d_n*/*d_c* values acquired *via* off-line analysis (*D* = *M_w*/*M_n*). Values listed are after 2 h of reaction time. ^c Total % conversion to cyclic carbonate observed *via* ¹H NMR spectroscopy after 2 h. Integration of methine signal peak areas for PPC (br, ~5.00 ppm) and PC (m, ~4.85 ppm) were used to determine % conversion. ¹H NMR spectra were collected in CDCl₃ at 298 K. ^d Calibrated using polystyrene standards (*d_n*/*d_c* = 0.185 mL g⁻¹).

based systems,^{32,33} and Fieser *et al.* saw full conversions to PC using a pyridine diimine cobalt catalyst system.³⁴ In most of these cases, high temperatures (up to 160 °C) and long-time scales (>20 h) were needed for high conversions to PC.

In the current work, depolymerization of PPC was performed using commercially available samples of PPC (~50 kDa, *D* = 3.93) under relatively mild conditions (75 °C ≤ *T* ≤ 105 °C, 2.5–10 mol% catalyst) using tris(pentafluorophenyl) borane (BCF) as a catalyst in toluene. Selective formation of PC was observed, and results are summarized in Table 1. A preliminary PPC depolymerization study was

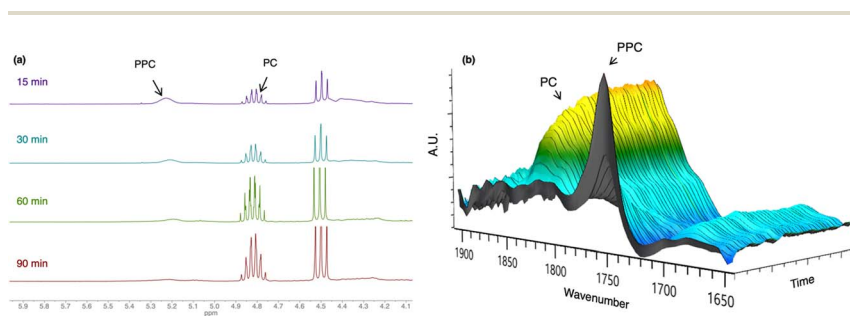


Fig. 1 (a) Stacked ¹H NMR spectra of aliquots taken for Table 1, entry 1 showing the formation of PC over time and (b) 3D FT-IR spectrum showing the formation of the cyclic carbonate peak (~1816 cm⁻¹) and disappearance of the polycarbonate peak (~1750 cm⁻¹) for Table 1, entry 6.



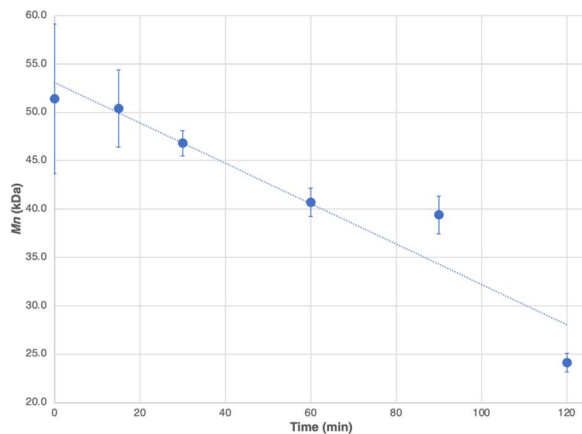


Fig. 2 Aliquot analysis by GPC of CDP of PPC (Table 1, entry 2) showing a linear decrease in M_n over time. Error bars are calculated from the Wyatt ASTRA Software report.

performed by Andrea *et al.* at 130 °C for 3 h with 5 mol% BCF in CH_2Cl_2 .¹³ Building on this work, toluene was chosen as the reaction solvent due to its higher boiling point and it being a relatively 'greener' solvent.^{35,36} It should be noted that recently the US EPA has determined CH_2Cl_2 to be an unreasonable risk to human health and therefore alternatives should be sought. The depolymerization of PPC at 5 mol% BCF at 105 °C (Table 1, entry 5) was tested and monitored *via* ^1H NMR spectroscopy and *in situ* FTIR spectroscopy (Fig. 1a and b, respectively), and gel permeation chromatography (GPC). To test if the solvent is necessary in this system, a solvent-free depolymerization was performed *via* ball mill grinding. After 1 h and 5 mol% BCF, no PC was observed *via* ^1H NMR spectroscopy. Similarly, liquid-assisted grinding (LAG) was attempted with 1 mL of toluene added to the grinding vessel. Again, no PC was observed *via* ^1H NMR spectroscopy indicating the necessity of polymer dissolution in a reaction solvent. Other researchers have successfully performed efficient depolymerizations of polymethacrylates,³⁷ poly(α -methyl styrene),³⁸ and PET,³⁹ in ball mills under solvent-free or LAG conditions. As expected, lowering the reaction temperature yields lower conversions of PPC to PC (Table 1, entries 1–5), as does lowering the catalyst loading (Table 1, entries 5–7). Analyses of aliquots *via* GPC shows a consistent decrease in molecular weights during the reaction, as seen in Fig. 2 for CDP with 5 mol% BCF at 95 °C (Table 1, entry 4).

The depolymerization of PPC was also tested with various impurities present to determine the behaviour of the system under non-ideal conditions. When using BCF that had been exposed to an ambient, lab atmosphere (air), ^1H NMR spectroscopic analysis evidenced no conversion to PC, indicating that BCF is too air and/or moisture sensitive to be an active depolymerization catalyst. Similarly, the reaction was tested with a large presence of CO_2 (40 bar). It was seen that the depolymerization was greatly hindered; only 15% conversion to PC was observed. This is likely due to CO_2 forming an adduct with BCF,¹² and reducing the number of active sites available for depolymerization. If an equal amount of PC (to PPC) is added to the system, PC formation is also hindered, yielding only a 70%

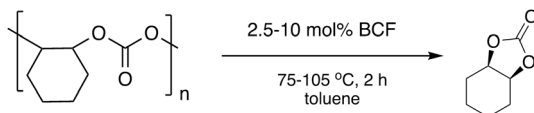


conversion (compared to a 92% conversion under the same conditions with no PC added) likely due to formation of Lewis-acid base complexes between PC and BCF (Fig. S6–S9†). Lastly, the depolymerization of a commercial polycarbonate diol was attempted to see the effect of the diol end-groups on the system. After 2 h, there was no conversion to PC seen by ^1H NMR spectroscopy, indicating the protic nature of the diol groups deactivates the BCF catalyst (Fig. S10†).

Depolymerization of poly(cyclohexene carbonate)

To date, most ROCOP systems for CO_2 /epoxide conversion test cyclohexene oxide (CHO) as a ‘proof of concept’ epoxide to form poly(cyclohexene carbonate) (PCHC) and to compare catalyst reactivities.^{12,13,17,20–23,40–47} When studying the CDP of PCHC, three potential products can be formed; *cis*-cyclohexene carbonate (*cis*-CHC), *trans*-cyclohexene carbonate (*trans*-CHC), and CHO (plus CO_2). PCHC is not available commercially and so it was prepared in our lab using BPh_3 with PPNCl, as described above. To achieve a fully circular chemical recycling to monomers (CRM), CHO and CO_2 are the desired products that can then re-enter the polymerization cycle and form new polymer. However, depending on the system, the energy barrier to CHO formation may be higher than CHC products.^{1,31,48} Recently, Williams and coworkers have reported a di- Mg^{II} catalyst that efficiently depolymerizes PCHC into CHO and CO_2 at 120 °C in 24 h,¹ and Yu *et al.* found a bimetallic Cr^{III} system that produces CHO and CO_2 from PCHC, at 110 or 150 °C in 1–24 h.⁸ While the formation of CHO is ideal for CRM, there are potential uses for CHC products.

Table 2 Cyclodepolymerization of PCHC after varying catalyst loading and temperature^a



Entry	BCF (mol%)	T (°C)	M_n (kDa) ^b	D	% CHC yield ^c
1	5	75	5.4	1.10	<1
2	5	85	4.2	1.05	<5
3	5	90	3.9	1.04	20
4	5	95	2.3	1.22	26
5 ^d	5	105	5.8	5.29	61
6	10	105	2.9	3.98	91
7	2.5	105	3.1	1.86	22

^a Conditions (unless otherwise stated): initial PCHC molecular weight (M_n) was measured to be 6.5 kDa ($D = 1.09$). Catalyst loadings were determined with respect to the repeat unit molar mass of the polymer. All reactions performed in 20 mL toluene for 2 h under nitrogen. ^b Molecular weights of aliquots determined by GPC in THF as the eluent. M_n and D were calculated using the Wyatt ASTRA software with d_n/d_c values acquired *via* off-line analysis ($D = M_w/M_n$). ^c Total % conversion to cyclic carbonate observed *via* ^1H NMR spectroscopy after 2 h. Integration of methine signal peak areas for PCHC (br, ~ 4.65 ppm) and CHC (m, ~ 4.54 ppm) were used to determine % conversion. ^1H NMR spectra were collected in CDCl_3 at 298 K. ^d Starting M_n was measured to be 8.3 kDa ($D = 1.09$).



Table 3 Depolymerization of terpolymers and polymer mixtures containing varying ratios of PCHC and PPC linkages^a

Entry	CHO : PO	% Conv. PCHC ^b	% Conv. PPC ^b
1	4 : 1	98	>99
2	1 : 2	>99	>99
3 ^c	4 : 1	70	70
4 ^c	1 : 1	62	59

^a All depolymerizations performed at 5 mol% BCF catalyst with respect to the repeat unit molar mass of PCHC. Performed in 20 mL toluene, at 105 °C for 2 h, under nitrogen.

^b Total % conversion to cyclic carbonate observed *via* ¹H NMR spectroscopy after 2 h. Integration of methine signal intensity for polycarbonate and cyclic carbonate was used to determine % conversion. ¹H NMR spectra were collected in CDCl₃ at 298 K.

^c Depolymerizations performed using mixtures of polycarbonates (PPC and PCHC) rather than terpolymers prepared from a mixture of PO, CHO, and CO₂.

CHC can be formed either directly from CHO and CO₂, or *via* CDP, dependent on conditions. Buchard *et al.* reported a bimetallic Fe^{III}/PPNCl ROCOP system that selectively produced *cis*-CHC from CHO and CO₂.⁴⁹ Darensbourg and coworkers observed that a metal-based (salen)CrCl catalyst could depolymerize PCHC to yield *trans*-CHC at 110 °C very slowly (full conversion after 170 h).³¹ Similar to the studies presented above with PPC, we report the CDP of PCHC using a BCF catalyst system, which selectively forms *cis*-CHC. These results are summarized in Table 2.

Compared to PPC, the depolymerization of PCHC was significantly slower, and did not form *cis*-CHC at temperatures lower than 85 °C, which aligns with the

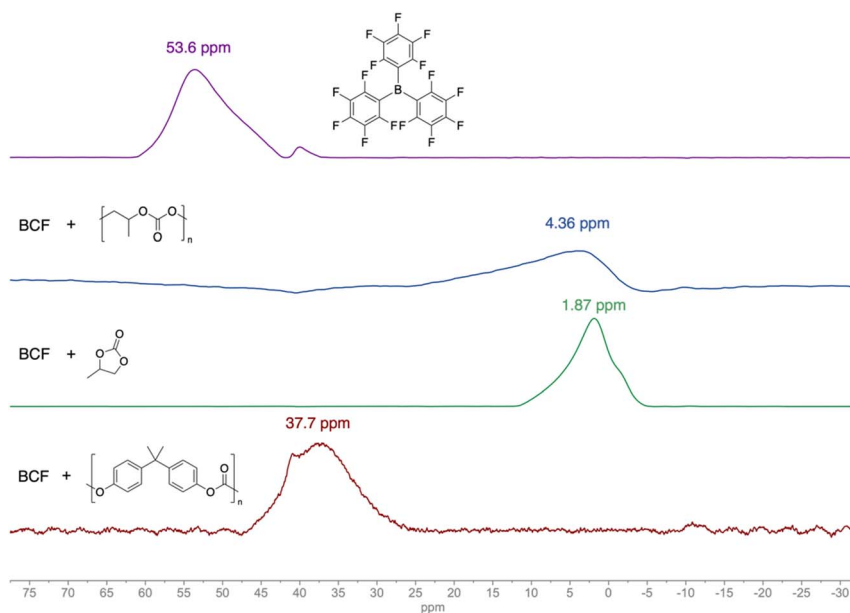
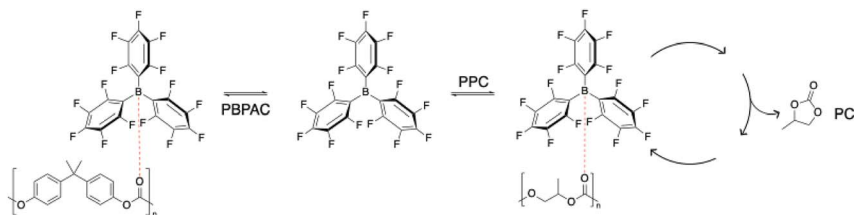


Fig. 3 ¹¹B NMR spectra (160 MHz, CDCl₃) of BCF alone (top, purple) and in the presence of PPC (second, blue), PC (third, green), or PBPAC (bottom, red).





Scheme 1 Representation of possible interactions between BCF and carbonate groups for the depolymerization of PBPAC and PPC mixture explaining slower CDP rates in the presence of two polycarbonates.

formation of a more thermodynamically strained bi-cyclic ring-containing product. When catalyst loadings are decreased, so is the conversion of PCHC to *cis*-CHC. Furthermore, the dispersities of PCHC during CDP show minimal broadening which implies a controlled mechanism is active. This will be discussed in more detail below. Interestingly, a lower molecular weight is seen by GPC in aliquots from reactions performed at 75 °C and 85 °C even when no cyclic carbonate formation is discernible *via* ^1H NMR spectroscopy. This implies that the polymer is slowly shortening in chain length even though the amount of cyclic carbonate is less than the detection limit of ^1H NMR spectroscopy.

Lastly, similar to the studies with PPC, the robustness of the system was tested with a 1 mol% water impurity present. After 2 h at 105 °C, <1% conversion of the polycarbonate was observed (Fig. S8†).

Terpolymer and polymer mixture depolymerizations

Previously, block terpolymers consisting of polyester and polycarbonate blocks were studied in the presence of BCF. It was seen that BCF selectively degraded the polycarbonate block and left the polyester block intact.¹³ Drawing upon this work, the depolymerizations of PPC and PCHC terpolymers were performed using the same conditions as the PPC or PCHC copolymer depolymerizations. These results are summarized in Table 3, entries 1 and 2. To compare, mixtures of polycarbonates (PPC and PCHC) containing similar ratios of the propylene carbonate and cyclohexene carbonate moieties to the terpolymers studied (Table 3, entries 3 and 4) were also investigated. Observations by ^1H NMR spectroscopy imply that the rate of CDP for PPC is slightly faster than PCHC when in a terpolymer, aligning with the FTIR spectroscopy studies presented herein. Comparing this to

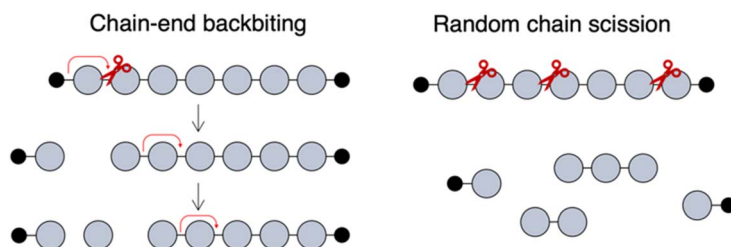


Fig. 4 Schematic of two possible CDP pathways presented in this work.^{31,50}



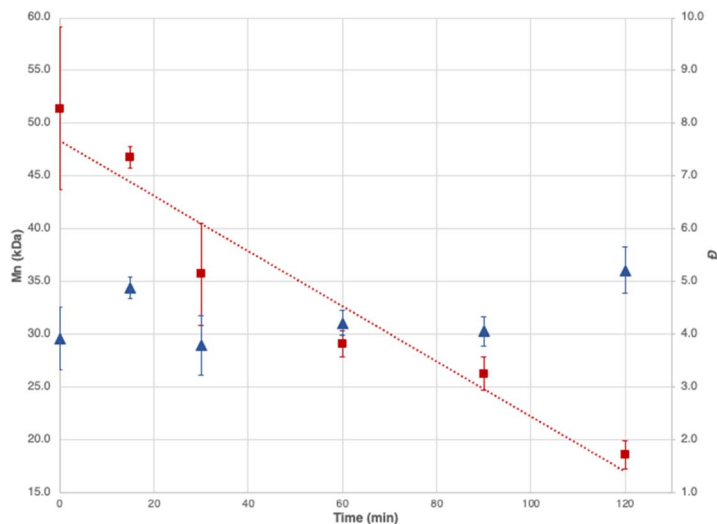


Fig. 5 Aliquot analysis by GPC of PPC (Table 1, entry 4) showing a linear decrease in M_n (red, squares) and minimal variation in D (blue, triangles). Error bars are calculated from the Wyatt ASTRA Software report.

a mixture of polycarbonates, the rate of cyclic carbonate formation seems to be slightly slower (by ^1H NMR spectroscopy). A possible explanation for this result may be the competition between the separate PCHC and PPC polymers to coordinate to the borane compared to the single chain block terpolymer.

Similarly, and inspired by work performed by Fieser and coworkers,³⁴ the depolymerization of an equal mixture of poly(bisphenol A) carbonate (PBPA)

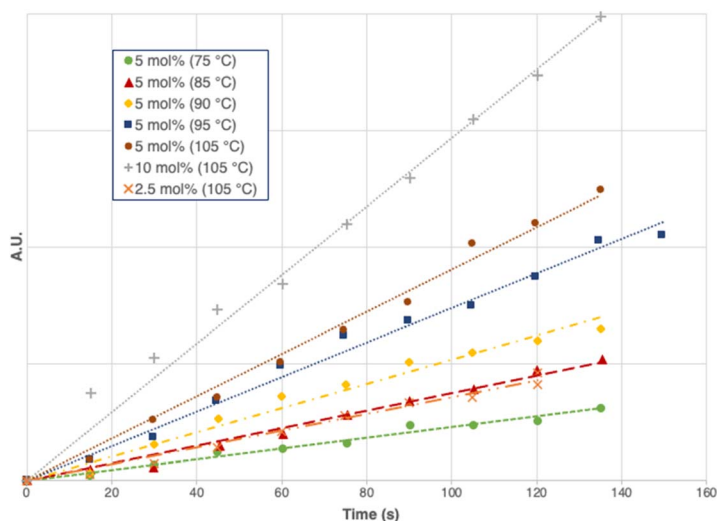


Fig. 6 Initial rates of cyclic carbonate formation taken from FTIR spectra around 1816 cm^{-1} . k_{app} values listed in Table 4 are taken from the slopes of the linear trendlines. R^2 values for all trends are >0.99 .



Table 4 Initial k_{apparent} values for cyclodepolymerization of PPC using BCF

Temperature (K)	k_{apparent} ($\text{s}^{-1} \times 10^{-5}$)
● 353	2.293
▲ 358	3.744
◆ 363	5.196
■ 368	7.784
● 378	9.033

and PPC was studied. First, a control reaction was performed with PBPAC (no PPC) to determine if BCF was a suitable catalyst for depolymerizing this widely used polycarbonate. No depolymerization was observed *via* ^1H NMR spectroscopy, likely due to the increased rigidity of this polymer and lack of a corresponding stable, small-ring cyclic carbonate product. When a 1 : 1 molar ratio of PBPAC and PPC was present, BCF selectively depolymerizes PPC into PC, albeit at a slightly slower rate than when only PPC is present (Fig. S14[†]). This may be due to interactions between the carbonate groups in PBPAC and the Lewis acidic boron centre in BCF. Interactions between boron and carbonate groups are evident in ^{11}B NMR spectroscopy studies as shown in Fig. 3 for PPC, PC, and PBPAC where significant shifts occur for the peak dependent on the species present. Interactions of the carbonate group of PBPAC with the boron centre can occur, blocking the active site, but the polymer does not undergo depolymerization. The PPC can displace the PBPAC at the boron centre and then enter the depolymerization cycle (Scheme 1).

Mechanistic studies

For the depolymerization to cyclic carbonates, two reaction mechanisms were considered: (1) chain-end backbiting, where the polymer unzips from the chain ends or (2) random chain scission, where the polymer is broken up at random to form shorter chains (Fig. 4).³³ To determine which is occurring in our system, the change in the polycarbonate molecular weight and dispersity were monitored over time *via* gel permeation chromatography (GPC) through reaction aliquot analysis. An exemplar trend of decrease in molecular weight (M_n) and dispersity (D) of PPC is shown in Fig. 5 (for Table 1, entry 4). A linear decrease in M_n paired with minimal variation in D points towards a chain-end backbiting depolymerization rather than degradation *via* random chain scission (Fig. 4), which would yield much higher D values *via* GPC.

Table 5 Initial k_{apparent} values for cyclodepolymerization of PCHC using BCF

Temperature (K)	k_{apparent} ($\text{s}^{-1} \times 10^{-5}$)	
+	358	0.5618
×	363	0.7484
●	368	0.8483
■	378	2.645



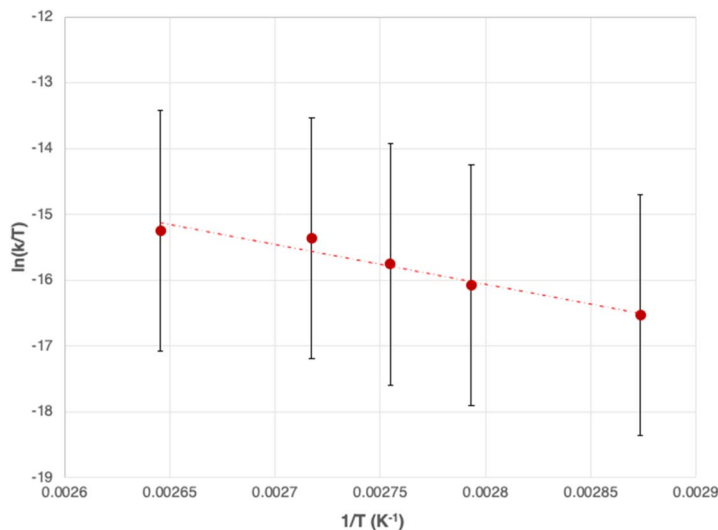


Fig. 7 Eyring plot of PPC CDP in toluene. $y = -6034x + 0.84$, $R^2 = 0.9496$. Error analysis performed as reported by Lente *et al.*⁵¹

Along the same lines, depolymerizations were monitored *via in situ* FTIR spectroscopy at varied temperatures and catalyst loadings to obtain reaction kinetic data. The polycarbonate peak ($\nu_{\text{CO}_2} = 1760 \text{ cm}^{-1}$) disappearance and cyclic carbonate ($\nu_{\text{CO}_2} = 1816 \text{ cm}^{-1}$) formation were observed. At lower temperatures, a possible induction period is observed, most likely due to the lower energy of the system. Apparent initial reaction rates were determined from the two-dimensional profiles of absorbance *vs.* time as a function of temperature

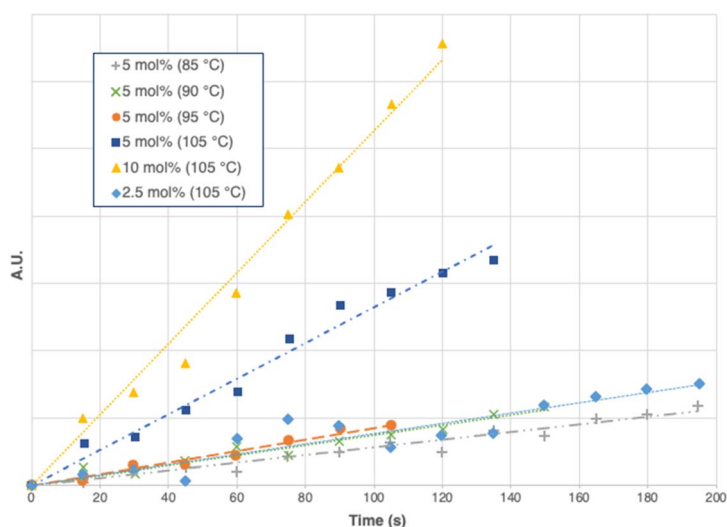


Fig. 8 Initial rates of cyclic carbonate formation during PCHC CDP taken from FTIR spectra at $\sim 1816 \text{ cm}^{-1}$. k_{app} values listed in Table 5 are taken from the slopes of the linear trendlines. R^2 values for all trends are >0.95 .



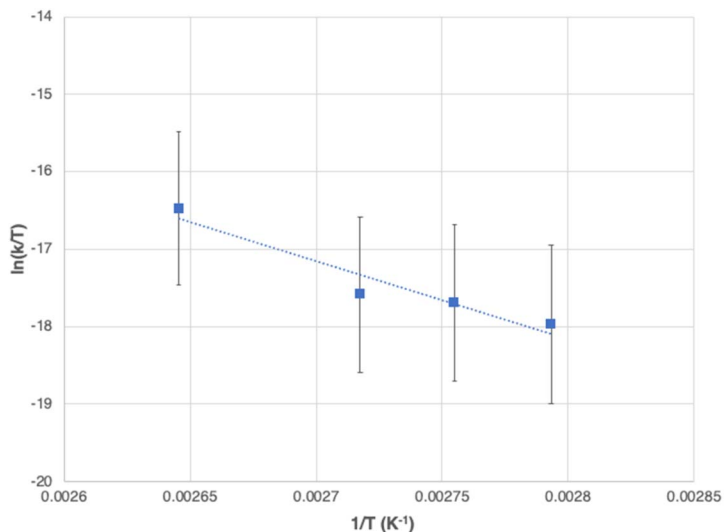


Fig. 9 Eyring plot of PCHC CDP in toluene. $y = -10045.6x + 1.0$, $R^2 = 0.9246$. Error analysis performed as reported by Lente *et al.*⁵¹

(Fig. 6) and are listed in Table 4. From these initial rates, the activation energies and entropies of the transition state can be calculated from the Eyring plots, illustrated in Fig. 7. The activation energy of PPC was found to be $50.2 \pm 6.8 \text{ kJ mol}^{-1}$ while the entropy of the transition state was revealed to be $-190.6 \pm 18.4 \text{ J K}^{-1} \text{ mol}^{-1}$ (Table 6). When compared to prior analyses, the energy of activation for PPC degradation ($50.2 \pm 6.8 \text{ kJ mol}^{-1}$) is lower than that reported for anion-assisted depolymerization catalyst systems ($80.5 \pm 3.6 \text{ kJ mol}^{-1}$).³¹ A

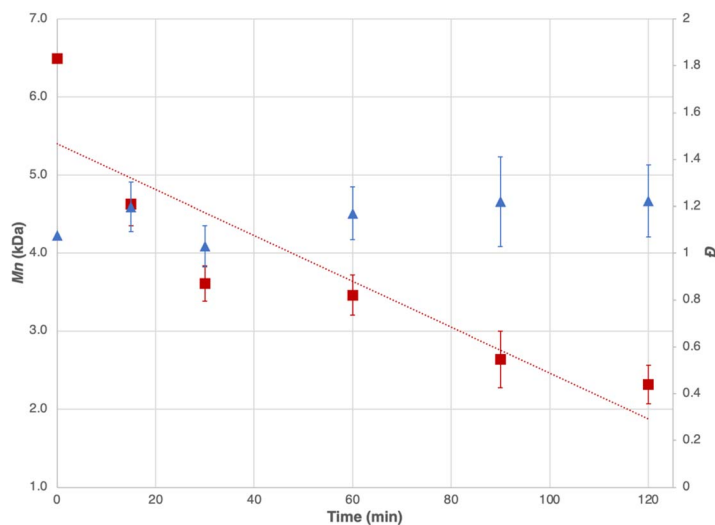


Fig. 10 Exemplar aliquot analysis of PCHC CDP reaction (Table 2, entry 4) by GPC showing linear decrease in M_n (red, squares) and variation in D (blue, triangles). Error bars are calculated from the Wyatt ASTRA Software report.



Table 6 Summary of activation parameters determined for CDP of PPC and PCHC^a

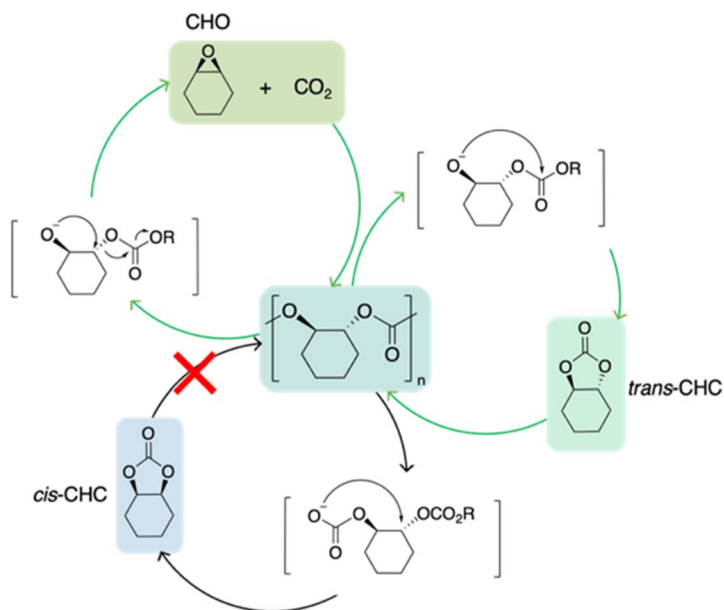
	ΔH^\ddagger (kJ mol ⁻¹)	ΔS^\ddagger (J K ⁻¹ mol ⁻¹)
PPC	50.2 ± 6.8	-190.6 ± 18.4
PCHC	83.5 ± 1.7	-114.7 ± 3.8

^a Values calculated from Eyring plots. Analysis performed *via* least squares regression. Error analysis performed as reported by Lente *et al.*⁵¹

transition state with a negative entropy value implies an associative depolymerization mechanism, where the borane centre is coordinated with the polymer chain. This is consistent with the previously mentioned ¹¹B NMR spectroscopy study and is most likely caused by an anionic polymer chain-end that coordinates to the borane. It is also important to note that in contrast to earlier research employing metal-centred complexes in combination with sources of anions (*e.g.* PPNN₃), in the current study, addition of such anions inhibits the reaction and BCF alone is effective in these CDP reactions.

The kinetic studies of PCHC were also performed using *in situ* FTIR spectroscopy (Fig. 8–10), yielding a higher activation energy and entropy of the transition state (83.5 ± 1.7 kJ mol⁻¹ and -114.7 ± 3.8 J K⁻¹ mol⁻¹, respectively, Table 6). A higher energy barrier is not surprising, considering the thermodynamic strain of the bicyclic product forming. Again, the apparent initial rates of reaction were calculated using the method described above. An induction period was also observed *via in situ* FTIR spectroscopy (Fig. S5†).

More varied M_n and \bar{D} trends were observed for the depolymerization of PPC with higher \bar{D} values (Fig. 5). This suggests a less controlled and different



Scheme 2 Possible CDP pathways for PCHC to form *cis*-CHC, *trans*-CHC, or CHO and CO₂.^{31,50}



depolymerization pathway for PPC, potentially with random chain scission occurring. Interestingly, higher D values were also observed for PCHC when higher catalyst loadings are employed. This implies a reduced amount of catalytic control in the system. At this point in the studies, we cannot determine if there may be two CDP pathways occurring concurrently *i.e.* chain-end and chain scission occurring on a single polymer chain.

As mentioned previously, the CDP of PCHC can form multiple products. The reaction pathways for each product are outlined in Scheme 2.^{31,50} ^1H NMR spectra yielding a multiplet at 4.63 ppm and the ν_{CO_2} stretching occurring at 1816 cm^{-1} in FTIR spectra indicates the selective formation of *cis*-CHC. If *trans*-CHC was observed, a multiplet would be seen *via* ^1H NMR at 3.90 ppm and the FTIR stretch would be visible around 1830 cm^{-1} .^{31,49} Buchard *et al.* saw *cis*-CHC as a product with their bimetallic Fe catalyst system for the addition of CHO and CO_2 , and proposed a double inversion of stereochemistry caused by the PPnCl co-catalyst.⁴⁹ Since no co-catalyst is used in this system, we propose the double inversion may occur due to the chloride end groups present on PCHC, which were previously confirmed by MALDI-TOF mass spectrometry.¹³

Conclusions

Further studies on the use of the highly Lewis acidic arylborane, BCF, as a cyclo-depolymerization catalyst for the degradation of CO_2 -based polycarbonates into cyclic products without the need for a co-catalyst are reported. Cyclic carbonates were formed from PPC and PCHC, with good conversions under relatively mild conditions. From mechanistic studies, the calculated activation energy and entropy of PPC CDP is lower than what was previously reported. For PCHC CDP, the energy and entropy of the transition state were calculated to be higher than that of PPC, but analysis *via* GPC and ^1H NMR spectroscopy implies a chain-end backbiting mechanism to selectively form *cis*-CHC. These results emphasize the potential for metal-free depolymerization catalyst systems that employ 'greener' conditions and can provide insight into more sustainable chemical polymer recycling strategies to useful products.

Data availability

The data supporting this article have been included as part of the ESI† or are presented within the article.

Author contributions

F. M. K., and M. D. W. conceived the idea for project. M. D. W. drafted the manuscript. M. D. W. performed experiments, characterization (NMR spectroscopy, *in situ* FTIR spectroscopy, and GPC), and data analysis. All authors have given approval to the final version of the manuscript.

Conflicts of interest

The authors declare no competing financial interest.



Acknowledgements

F. M. K. acknowledges financial support from Natural Sciences and Engineering Research Council of Canada (NSERC) for a Discovery and a CREATE Grant, Memorial University, the Canada Foundation for Innovation, and the Government of Newfoundland and Labrador. M. D. W. thanks NSERC for a Canada Graduate Scholarship (Doctoral) and Memorial University for Dr Liqin Chen Graduate Scholarships. We thank Memorial University's CREAT Network for their support with this work.

References

- 1 F. N. Singer, A. C. Deacy, T. M. McGuire, C. K. Williams and A. Buchard, *Angew. Chem., Int. Ed.*, 2022, **61**, e202201785.
- 2 T. Keijer, V. Bakker and J. C. Slootweg, *Nat. Chem.*, 2019, **11**, 190–195.
- 3 Canada Plastics Pact, *Canada-Wide Plastic Packaging Flows: A 2024 Progress Report*, Generate Canada, 2024.
- 4 United Nations Development Programme, Plastics 101, <https://www.undp.org/plastics-101>, accessed April 11, 2025.
- 5 K. Ragaert, L. Delva and K. Van Geem, *Waste Manag.*, 2017, **69**, 24–58.
- 6 A. C. Deacy, C. B. Durr and C. K. Williams, *Dalton Trans.*, 2020, **49**, 223–231.
- 7 M. L. Smith, T. M. McGuire, A. Buchard and C. K. Williams, *ACS Catal.*, 2023, **13**, 15770–15778.
- 8 Y. Yu, B.-H. Ren, Y. Liu and X.-B. Lu, *ACS Macro Lett.*, 2024, **13**, 1099–1104.
- 9 G.-W. Yang, Y. Wang, H. Qi, Y.-Y. Zhang, X.-F. Zhu, C. Lu, L. Yang and G.-P. Wu, *Angew. Chem., Int. Ed.*, 2022, **61**, e202210243.
- 10 C. Shi, W. T. Diment and E. Y.-X. Chen, *Angew. Chem., Int. Ed.*, 2024, **63**, e202405083.
- 11 T. M. McGuire, A. C. Deacy, A. Buchard and C. K. Williams, *J. Am. Chem. Soc.*, 2022, **144**, 18444–18449.
- 12 K. A. Andrea and F. M. Kerton, *ACS Catal.*, 2019, **9**, 1799–1809.
- 13 K. A. Andrea, M. D. Wheeler and F. M. Kerton, *Chem. Commun.*, 2021, **57**, 7320–7322.
- 14 K. A. Andrea, H. Plommer and F. M. Kerton, *Eur. Polym. J.*, 2019, **120**, 109202.
- 15 K. Andrea and F. Kerton, *RSC Adv.*, 2019, **9**, 26542–26546.
- 16 Z. Chen, J.-L. Yang, X.-Y. Lu, L.-F. Hu, X.-H. Cao, G.-P. Wu and X.-H. Zhang, *Polym. Chem.*, 2019, **10**, 3621–3628.
- 17 V. K. Chidara, S. K. Boopathi, N. Hadjichristidis, Y. Gnanou and X. Feng, *Macromolecules*, 2021, **54**, 2711–2719.
- 18 C. Zhang, X. Geng, X. Zhang, Y. Gnanou and X. Feng, *Prog. Polym. Sci.*, 2023, **136**, 101644.
- 19 G.-W. Yang, C.-K. Xu, R. Xie, Y.-Y. Zhang, X.-F. Zhu and G.-P. Wu, *J. Am. Chem. Soc.*, 2021, **143**, 3455–3465.
- 20 J. Zhang, L. Wang, S. Liu, X. Kang and Z. Li, *Macromolecules*, 2021, **54**, 763–772.
- 21 D. Zhang, S. Boopathi, N. Hadjichristidis, Y. Gnanou and X. Feng, *J. Am. Chem. Soc.*, 2016, **138**, 11117–11120.
- 22 J. Schaefer, H. Zhou, E. Lee, N. S. Lambic, G. Culcu, M. W. Holtcamp, F. C. Rix and T.-P. Lin, *ACS Catal.*, 2022, **12**, 11870–11885.



- 23 R. Xie, Y. Wang, S. Li, B. Li, J. Xu, J. Liu, Y. He, G.-W. Yang and G.-P. Wu, *Angew. Chem., Int. Ed.*, 2024, **63**, e202404207.
- 24 G. Yang, Y. Zhang, R. Xie and G. Wu, *J. Am. Chem. Soc.*, 2020, **142**, 12245–12255.
- 25 L.-F. Hu, D.-J. Chen, J.-L. Yang and X.-H. Zhang, *Molecules*, 2020, **25**, 253.
- 26 J. Liu, Y. Gnanou and X. Feng, *Macromolecules*, 2022, **55**, 1800–1810.
- 27 C.-J. Zhang, S.-Q. Wu, S. Boopathi, X.-H. Zhang, X. Hong, Y. Gnanou and X.-S. Feng, *ACS Sustain. Chem. Eng.*, 2020, **8**, 13056–13063.
- 28 M. Zhao, S. Zhu, G. Zhang, Y. Wang, Y. Liao, J. Xu, X. Zhou and X. Xie, *Macromolecules*, 2023, **56**, 2379–2387.
- 29 W. Kuran and P. Górecki, *Makromol. Chem.*, 1983, **184**, 907–912.
- 30 W. Kuran and T. Listoś, *Macromol. Chem. Phys.*, 1994, **195**, 1011–1015.
- 31 D. J. Darensbourg and S.-H. Wei, *Macromolecules*, 2012, **45**, 5916–5922.
- 32 C. Alberti, D. Rijono, M. Wehrmeister, E. Cheung and S. Enthaler, *ChemistrySelect*, 2022, **7**, e202104004.
- 33 C. F. Gallin, W.-W. Lee and J. A. Byers, *Angew. Chem., Int. Ed.*, 2023, **62**, e202303762.
- 34 K. D. Knight and M. E. Fieser, *Inorg. Chem. Front.*, 2024, **11**, 298–309.
- 35 F. P. Byrne, S. Jin, G. Paggiola, T. H. M. Petchey, J. H. Clark, T. J. Farmer, A. J. Hunt, C. Robert McElroy and J. Sherwood, *Sustain. Chem. Process.*, 2016, **4**, 7.
- 36 L. J. Diorazio, D. R. J. Hose and N. K. Adlington, *Org. Process Res. Dev.*, 2016, **20**, 760–773.
- 37 E. Jung, M. Cho, G. I. Peterson and T.-L. Choi, *Macromolecules*, 2024, **57**, 3131–3137.
- 38 E. Jung, D. Yim, H. Kim, G. I. Peterson and T. Choi, *J. Polym. Sci.*, 2023, **61**, 553–560.
- 39 V. Štrukil, *ChemSusChem*, 2021, **14**, 330–338.
- 40 Y. C. A. Sokolovicz, A. Buonerba, C. Capacchione, S. Dagorne and A. Grassi, *Catalysts*, 2022, **12**, 970.
- 41 W. T. Diment, W. Lindeboom, F. Fiorentini, A. C. Deacy and C. K. Williams, *Acc. Chem. Res.*, 2022, **55**, 1997–2010.
- 42 D. R. Moore, M. Cheng, E. B. Lobkovsky and G. W. Coates, *J. Am. Chem. Soc.*, 2003, **125**, 11911–11924.
- 43 B. Han, B. Liu, H. Ding, Z. Duan, X. Wang and P. Theato, *Macromolecules*, 2017, **50**, 9207–9215.
- 44 K. Ni and C. M. Kozak, *Inorg. Chem.*, 2018, **10**, 3097–3106.
- 45 G. Sulley, G. Gregory, T. Chen, L. Carrodegua, G. Trott, A. Santmarti, K. Lee, N. Terrill and C. Williams, *J. Am. Chem. Soc.*, 2020, **142**, 4367–4378.
- 46 J. Huang and B. Shen, *Polym. Chem.*, 2024, **15**, 4519–4528.
- 47 G. Rosetto, F. Vidal, T. M. McGuire, R. W. F. Kerr and C. K. Williams, *J. Am. Chem. Soc.*, 2024, **146**, 8381–8393.
- 48 D. J. Darensbourg, A. D. Yeung and S.-H. Wei, *Green Chem.*, 2013, **15**, 1578.
- 49 A. Buchard, M. R. Kember, K. G. Sandeman and C. K. Williams, *Chem. Commun.*, 2010, **47**, 212–214.
- 50 G. W. Coates and Y. D. Y. L. Getzler, *Nat. Rev. Mater.*, 2020, **5**, 501–516.
- 51 G. Lente, I. Fábíán and A. J. Poč, *New J. Chem.*, 2005, **29**, 759.

